352295
N95-14573

# DYNAMICS OF HARD SPHERE COLLOIDAL DISPERSIONS

J.X. Zhu and P.M. Chaikin
Department of Physics

S.-E. Phan and W.B. Russel
Department of Chemical Engineering
Princeton University
Princeton NJ 08544

## INTRODUCTION

One of the most fundamental systems in nature is that of hard spheres, particles that do no interpenetrate but otherwise do not overlap. Hard spheres display many of the thermodynamic, hdyrodynamic, and transport properties of both molecular and colloidal systems, including transitions from disordered fluid to crystalline solid or disordered glasslike states and a host of nonideal static and dynamic phenomena. Physical realization of this most basic of interacting systems is possible with the inert gases only at extreme temperatures or pressures, but several well-studied colloidal particles provide very faithful approximations and are amenable to study at convenient length and time scales through dynamic and static light scattering. The synthesis of monodisperese spheres, stabilization by repulsions of range short relative to the radius, and index matching in organic solvents to minimize van der Waals attraction snd multiple scattering provides convincing hard sphere behavior over moderate time scales [1,2]. However, experiments with equilibration times of of days to weeks, such as crystallization, suffer from sedimentation due to the density difference between the solvent and particles [3].

The specific shortcomings of existing studies pertain primarily to the disorder-order transition, a subtle entropy driven process that leads to coexistence between a disordered phase with liquid-like order at a volume fraction $\phi$=0.494 and a face-centered-cubic solid at $\phi$=0.545. Experiments confirm fairly well the phase boundaries and suggest a glass transition at $\phi$=0.56-58, but detect a crystal structure more closely described by random stacking of hexagonally packed layers [4]. In addition, small angle light scattering studies of crystal growth do not yield the form factors expected for the linear growth of uncorrelated crystallites, but a considerably more complex form [5]. Either or both of these could arise from subtle effects of gravitational settling, which produces settling velocities comparable to diffusion velocities early in the process of nucleation and growth of crystallites. Furthermore, the equilibrium state under gravity consists of an almost closepacked, inhomogeneous crystal or glass, far from the homogeneous sample desired.

So our objective is to perform on homogeneous, fully equilibrated dispersions the full set of experiments characterizing the transition from fluid to solid and the properties of the crystalline and glassy solids. These include measurements quantifying the nucleation and growth of crystallites, the structure of the initial fluid and the fully crystalline solid, the Brownian motion of particles within the crystal, and the elasticity of the crystal and the glass. Experiments are being built and tested for the ideal microgravity environment. Here we describe the ground based effort, which exploits a fluidized bed to create a homogeneous, steady state dispersion for the studies. The difference between the microgravity environment and the fluidized bed is gauged by the Peclet number Pe, which measures the rate of convection/sedimentation relative to Brownian motion.

We have designed our experiment to accomplish three types of measurements on hard sphere suspensions in a fluidized bed: the static scattering intensity as a function of angle to determine the structure factor, the temporal autocorrelation function at all scattering angles to probe the dynamics, and the amplitude of the response to an oscillatory forcing to deduce the low frequency viscoelasticity. Thus the scattering instrument and the colloidal dispersion were chosen such that the important features of each physical property lie within the detectable range for each measurement.

## COLLOIDAL DISPERSION

Our colloidal system consists of highly monodisperse poly(methyl methacrylate) (PMMA) particles with a layer of covalently bound poly(12 hydroxy stearic acid) (PHSA) chains. The branched PHSA chains provide a sufficiently thick layer (9-10 nm) to reduce the van der Waals attraction below the thermal energy, leaving as the dominant interaction a slightly soft, or nearly hard, repulsion when the polymer layers of different particles interact. PMMA/PHSA dispersions comprise a widely accepted and extensively documented model system for investigating hard sphere behavior [6,7,8].

The particles were synthesized in the laboratory of R.H. Ottewill by a one-shot (batch) dispersion polymerization [9]. This modified precipitation polymerization depends on the monomer (methyl methacrylate, MMA) being soluble in the dispersion medium while its polymer is not. The solvency of the dispersion medium controls the particle size, i.e. high monomer concentrations produce large particles. In this case, the medium consisted of hexane (aromatic free), dodecane, 40/60 petroleum ether, and a high boiling hydrocarbon. The comb stabilizer was prepared as a graft copolymer of PHSA with PMMA. Heating the monomer, stabilizer, and dispersion medium in an Ehrlenmeyer flask to 80°C initiated nucleation and growth of the particles. After completion of growth a further reaction covalently linked the backbone of the stabilizer to the particle. Excess stabilizer was removed by repeated centrifugation, removal of the supernatant, and redispersion in dodecane. Later we later replaced the dodecane with a more suitable solvent by a similar procedure.

Matching the refractive index of the PMMA (n=1.5240) with that of the solvent prevents multiple scattering and suppresses van der Waals forces. Combining a mixture of cis- and trans-1,2,3,4-decahydronapthalene (decalin with n=1.4750) with 1,2,3,4-tetrahydronapthalene (tetralin with n=1.5410) in the proper proportion accomplishes the match, as judged qualitatively by the clear appearance of the dispersion and quantitatively by a minimum in the intensity of scattered laser light. For the particles discussed here, with a nominal diameter of 1000 nm, the index matching solvent consists of 74.2% tetralin and 25.8% decalin with refractive index n=1.5240 for the sodium line at 25°C. For sedimentation of these particles in this solvent mixture at 25°C Pe=0.2. Whether this is sufficiently small not to affect the equilibrium remains to be seen.

## FLUIDIZED BED AND SCATTERING INSTRUMENT

The fluidized bed consists of a uniform glass NMR tube with 13 mm ID and 1 mm wall thickness and a distributer consisting of a 0.2 μm membrane filter mounted at the bottom. Flow is controlled by a syringe pump (Harvard Apparatus Model 33). The membrane retains the PMMA spheres in the tube as the syringe pump drives fluid flow upwards to offset sedimentation due to the density mismatch between the particles (~1.1 g/cm$^3$) and the fluid (~0.95 g/cm$^3$). Therefore, in the laboratory reference frame, the dispersion is static at a volume fraction set by the fluid velocity and the volume fraction dependence of the settling velocity. At the superficial velocity of 63 μm/day set here the colloidal suspension is fully crystalline, i.e. at a volume fraction above 0.55.

The light scattering part of the apparatus is shown in Figure 1. An Argon ion laser operating at 488 nm wavelength is stabilized with a power controller that limits the peak-to-peak fluctuations to within 0.2% of the average intensity, allowing measurements of the intensity temporal autocorrelation function to below $10^{-4}$ of the baseline. The incident laser beam passes through the center of a cylindrical glass vat (32 cm diameter) filled with a hydrocarbon oil that approximately matches the index of the dispersion. The fluidized bed of PMMA particles is located at the center of the vat and aligned at the center of a goniometer. To ensemble average the intensities, as required for non-ergodic systems such as colloidal glasses or crystals [10], we translate the fluidized bed vertically and rotate independently about the axis, via stages driven by computerized DC servo motors.

The scattered light is detected at any desired angle by a photon multiplier tube (Hamamatsu H4730-01 PMT and Amplifier/Discriminator Assembly) through optics mounted on an arm that rotates with the goniometer. The detection optics consist of a lens that images the scattering volume to the photo cathode of the PMT and two apertures, the first (2 mm diameter) mounted immediately in front of the lens to limit the acceptance angle to 0.8° and the second (50 μm diameter) to define the scattering volume. The size of the latter compares with the speckle size of the scattered light. The signal is collected by a digital correlator [ALV 5000] which constructs the temporal autocorrelation function and computes the static intensity. To probe the structure factor at low angles, we use a CCD camera [GBC CCD-500E] to capture the intensity pattern of a screen glued to the outside of the vat.

The shear modulus and viscosity of the hard sphere dispersion are detected through so-called Bragg spectroscopy. A function generator produces a sinusoidal voltage to drive a speaker attached to the rotational stage holding the fluidized bed, thereby gently rotating it at a prescribed frequency and creating an oscillatory disturbance within the dispersion. When the amplitude of the oscillation is small relative to the inverse of the scattering wavevector, the scattered intensity fluctuates at the same frequency, and the ensemble averaged temporal autocorrelation function of the scattered intensity from the center of the bed indicates the amplitude of response. The rheological properties are then extracted by modelling the colloidal system as a linear viscoelastic solid.

## RESULTS AND DISCUSSION

The scattering intensity pattern from the fluidized bed at low angles is shown in Figure 2 with the incident beam directed normal and into the photo but blocked by a vertical stop at the center. The Bragg scattering from the crystalline dispersion forms five symmetric rings on each side. We list the Bragg angles in Table 1 along with the

ratio of the scattering wavevector at the particular Bragg angles, q, to that of the first Bragg angle. For comparison columns 3 and 4 list the corresponding face-centered cubic (fcc) planes and the ratio of the reciprocal lattice vector G to that of the (1,1,1) plane, whereas column 5 lists the ratios for the randomly stacked hexagonal (rsh) planes.

Table 1: Comparison of Bragg angles with those expected for fcc and rsh crystals

| Bragg angle [°] | $q/q_1$ | fcc planes | $G/G_{111}$(fcc) | $G/G_{111}$(rsh) |
|---|---|---|---|---|
| 17.9 | 1 | (1,1,1) | 1 | 1 |
| 20.8 | 1.1604 | (2,0,0) | 1.154701 | — |
| 29.4 | 1.6311 | (2,2,0) | 1.632993 | 1.632993 |
| 34.6 | 1.9115 | (3,1,1) | 1.914854 | 1.914854 |
| 36.3 | 2.0023 | (2,2,2) | 2 | 2 |

The table indicates an fcc structure for the hard sphere crystal in the fluidized bed, since the ratios of the scattering wavevectors match all lines for the fcc crystal. However, the intensity of the second Bragg peak is much less than the first one, suggesting that some crystal grains may have rsh structures which contribute to the intensity of all but the second peak. Thus the structure observed may be a mixture of face-center-cubic and randomly stacked hexagonal crystallites. Assessing the relative amounts requires quantitative analysis of the intensities, which is now underway.

Proper interpretation of dynamic light scattering from colloidal crystals requires ensemble averaged temporal autocorrelation functions, since particles are localized in the vicinity of their lattice points. The scattered intensity has fixed and fluctuating components, so time averaging does not suffice. To solve this problem, we averaged autocorrelation functions measured at many different positions separated by 50 μm, the dimension of the scattering volume. Typical temporal autocorrelation functions averaged over 500 positions in Figure 3 exhibit the expected spread, e.g. about 4.2% at longer times as compared with $1/(500)^{1/2}$=4.5%. Thus, in order to achieve accuracy better than 1%, we must measure autocorrelation function at 10,000 positions.

To relate these measurements to the dynamics of particles within the crystal, we adopt a simple model from solid state physics that considers only random motion about the lattice points with no correlation between different particles. This model leads to an autocorrelation function containing two terms. The first comprises the dynamic structure factor, reflecting the correlation of particle positions with the lattice site, and decays to zero at long times. The second is the self-dynamic structure factor, resulting from the polydispersity in the index of refraction of particles, and decaying to a finite value reflecting the limited volume available to each particle. Clearly the prediction conforms qualitatively to the observations. Quantitative fits of the functional form predicted to the observed autocorrelation functions should determine whether the model is sufficient and, if so, magnitudes of the short-time self diffusion coefficient and maximum mean square displacement for particles within the crystal. The former might then be compared with values for the metastable fluid phase at the same volume fraction and the latter with the maximum displacement expected for a crystal from the Lindemann criterion.

## SUMMARY

In summary, we have assembled an instrument capable of measuring the structure, dynamics, and rheological properties of colloidal crystals in a homogeneous fluidized state. Preliminary experiments produced a hard sphere colloidal polycrystal with a mixture of face-centered cubic and random stacked hexagonal layer domains. Dynamic measurements confirm the need to ensemble average to obtain useful autocorrelation functions and suggest non-decaying fluctuations.

## ACKNOWLEDGEMENTS

This work was supported by the National Aeronautics and Space Administration - Microgravity Fluid Dynamics and Transport Phenomena through grant no. NAG3-1158. The authors thank Professor B.J. Ackerson for providing the PMMA sample.

1. C.G. de Kruif, J.W. Jansen, and A. Vrij, *Physics of Complex and Supramolecular Fluids* (ed. S. Safran and N.A. Clark) Wiley, p. 315 (1986).

2. P.N. Pusey and W. van Megen, *Physics of Complex and Supramolecular Fluids* (ed. S. Safran and N.A. Clark) Wiley, p. 673 (1986); *Nature* **320** 340 (1986).

3. S.E. Paulin and B.J. Ackerson, *Phys. Rev. Lett.* **64** 2663 (1990).

4. P.N. Pusey, W. van Megen, P. Bartlett, B.J. Ackerson, J.G. Rarity, and S.M. Underwood, *Phys. Rev. Lett.* **63** 2753 (1989).

5. D.J.W. Aastuen, N.A. Clark, J.C. Swindal, and C.D. Muzney, *Phase Trans.* **21** 139 (1990); K. Schatzel and B.J. Ackerson, *Phys. Rev. Lett.* **68** 337 (1992).

6. P. Bartlett, R.H. Ottewill, and P.N. Pusey, *J. Chem. Phys.* **93** 1299 (1990).

7. W.B. Russel, D.A. Saville, and W.R. Schowalter, *Colloidal Dispersions* Cambridge, Chap 14 (1989).

8. J.W. Goodwin and R.H. Ottewill, J. *Chem. Soc. Far. Trans.* **87** 357 (1991).

9. L. Antl, J.W. Goodwin, R.D. Hill, R.H. Ottewill, S.M. Owens, and S. Papworth, *Colloids Surf.* **17** 67 (1986).

10. P.N. Pusey and W. van Megen, *Physica A* **157** 705 (1989).

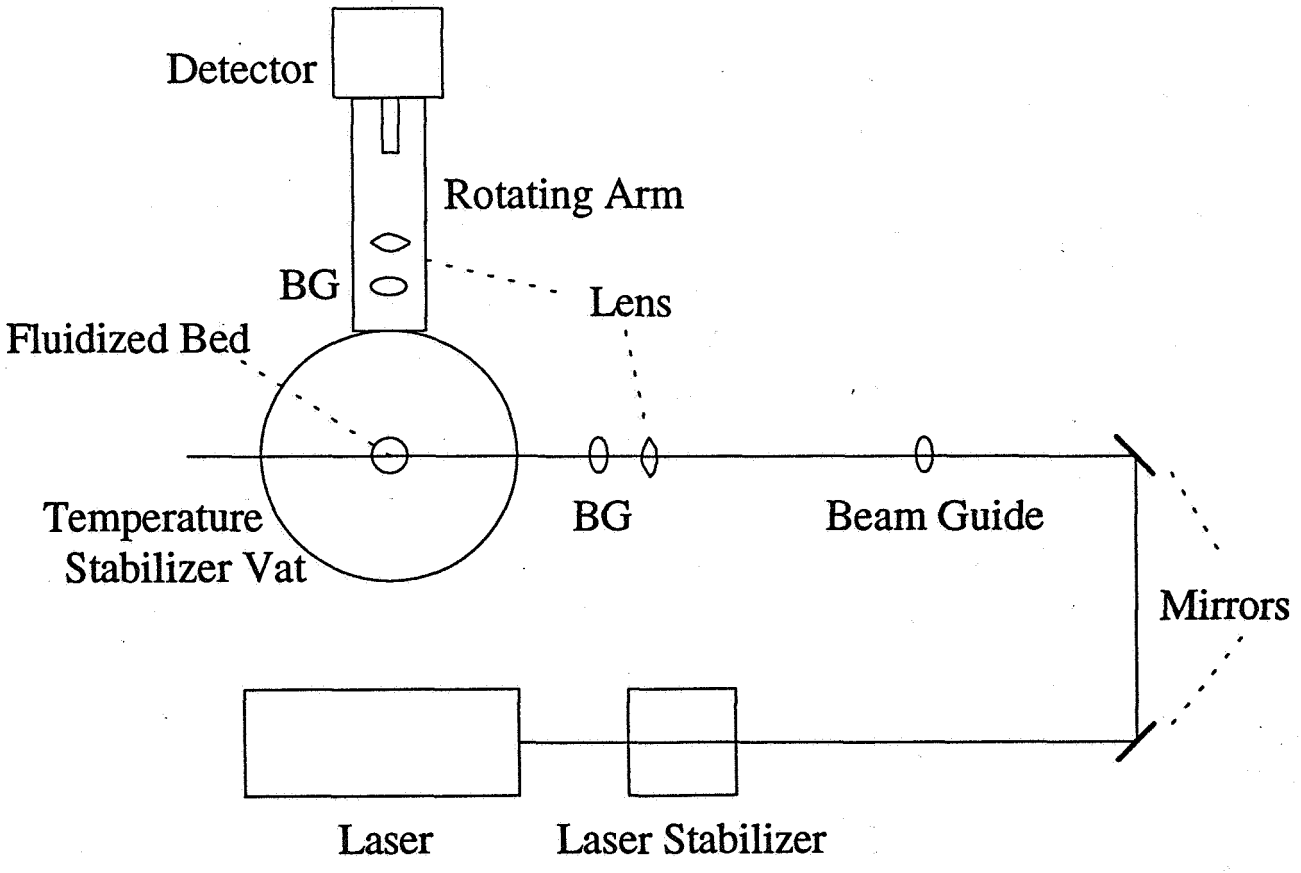


Figure 1 - Light scattering apparatus

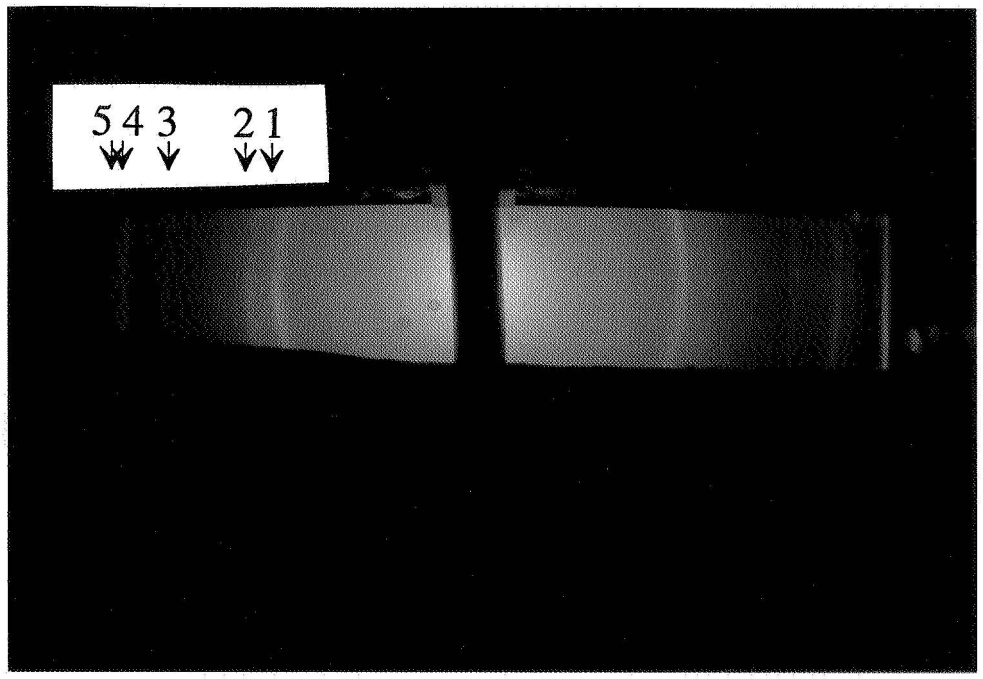


FIgure 2 - Photograph of Bragg diffraction rings from dispersion of 1000 nm PMMA spheres in decalin/tetralin mixture projected onto screen attached to vat: 1 - 111, 2 - 200, 3 - 220, 4 - 311, 5 - 222.

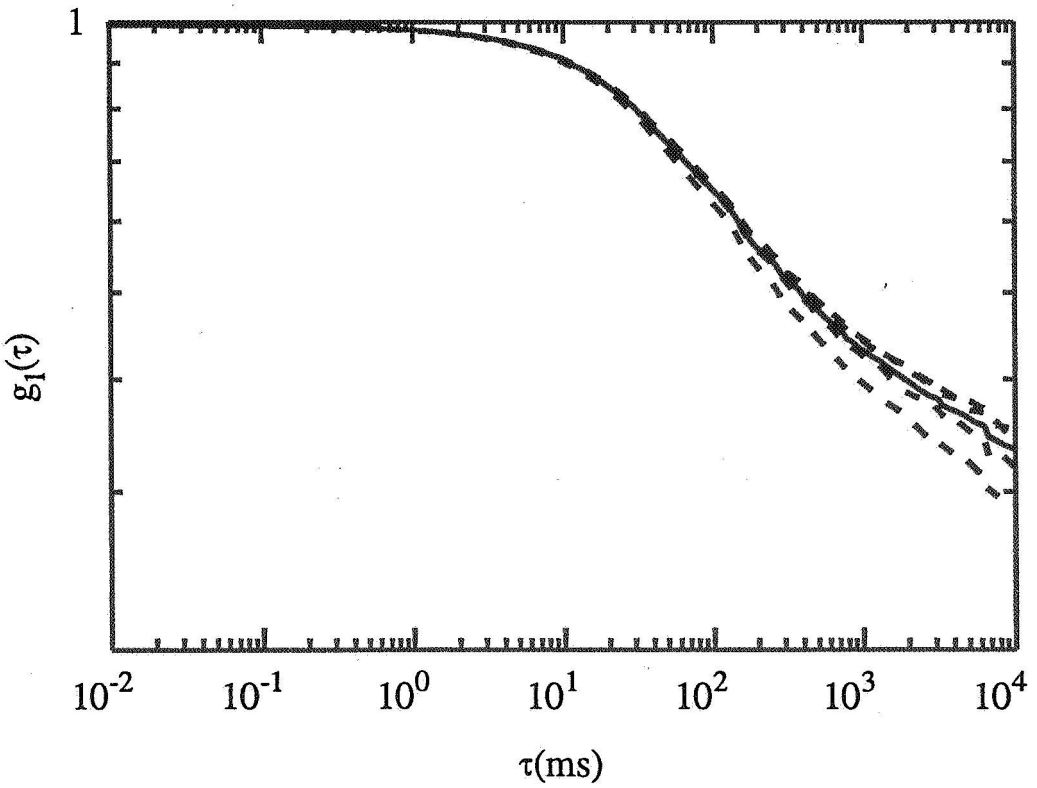


Figure 3 - Temporal autocorrelation function at 110° with 1000 nm PMMA spheres in decalin/tetralin mixture averaged over four different sets of 500 positions (- - - ) and all 2000 positions (------).